Article

The Role of Dendritic Cells in Adaptive Immune Response Induced by Ova/Pdda Nanoparticles

Daniele R. Pereira , Yunys Pérez-Betancourt , Bianca C. L. F. Távora , Geraldo S. Magalhaes , Ana Maria Carmona-Ribeiro , Eliana L. Faquim-Mauro *

Posted Date: 1 November 2024

doi: 10.20944/preprints202411.0114.v1

Keywords: nanoparticles; Poly-diallyl-dimethyl-ammonium chloride (PDDA); dendritic cell; adjuvant; immune response; vaccine

 doi:10.20944/preprints202411.0114.v1

Article

The Role of Dendritic Cells in Adaptive Immune Response Induced by OVA/PDDA Nanoparticles

Daniele R. Pereira [1,2], Yunys Perez-Betancourt [3], Bianca C. L. F. Távora [1,2], Geraldo S. Magalhães [1], Ana Maria Carmona-Ribeiro [3] and Eliana L. Faquim-Mauro [1,2,*]

[1] Laboratory of Immunopathology, Butantan Institute, São Paulo, Brazil
[2] Department of Immunology, Institute of Biomedical Sciences, University of São Paulo, São Paulo, Brazil
[3] Department of Biochemistry, Chemistry Institute, University of São Paulo, São Paulo, Brazil
* Correspondence: eliana.faquim@butantan.gov.br; Tel.: +(55)(11) 2627-9783

Abstract: Cationic polymers were previously shown to assemble with negatively charged proteins yielding nanoparticles (NPs). Poly-diallyl-dimethyl-ammonium chloride (PDDA) is a cationic polymer able to combine with ovalbumin (OVA) yielding a stable colloidal dispersion of OVA/PDDA NPs eliciting significant anti-OVA immune response. Dendritic Cells (DC), as sentinels of foreign antigens, exert a crucial role in the induction of antigen-specific T cell activation and consequent adaptive immune response. **Objective:** The present study aimed at evaluating the involvement of DCs in the adaptive immune response induced by OVA/PDDA. **Methods/Results:** Confirming the potent induction of adaptive immune response against OVA/PDDA, the data showed increased $CD19^+CD138^+$ plasma cells and $CD19^+CD38^+CD27^+$ memory cells in spleens of mice immunized with OVA/PDDA-NPs 28 days before. OVA/PDDA-NPs also induced the migration and maturation of DCs to draining lymph nodes on days 3 and 4 of mice immunization. The *in vitro* results with bone-marrow differentiated DCs (iBM-DCs) showed an increase of the binding and uptake of OVA/PDDA NPs by these cells compared with soluble OVA. In addition, OVA/PDDA NPs were able to induce DC maturation and upregulation of costimulatory and MHC-II molecules, TNF-α and IL-12 production. iBM-DCs incubated with OVA/PDDA NPs promoted high OVA-specific T cell proliferative response. **Conclusion:** Altogether, the data demonstrated the central role of DCs in the induction of antigen-specific immune response by OVA-PDDA-NPs, thus proving these NPs as potent adjuvants for subunit vaccine design.

Keywords: nanoparticles; Poly-diallyl-dimethyl-ammonium chloride (PDDA); dendritic cell; adjuvant; immune response; vaccine

1. Introduction

The induction of protective immune responses against different pathogens including different viruses, as well as cancer has been a difficult challenge for the scientific community [1–4]. In this sense, distinct strategies have been designed to promote the appropriate immune system activation with the goal of inducing enhanced memory immunity to protect against future pathogen infections [2,5]. Neutralizing antibodies produced by B cells and T lymphocyte responses mediate the mechanisms of protection against pathogens induced by vaccines [3]. In the induction of protective response against distinct pathogens, subsets of $CD4^+$ T cells provide help for B cell development and antibody production in lymphoid tissues [6] and also the generation of memory immunity. $CD8^+$ T cell response is also induced during the immune system activation by infection or vaccination and $CD8^+$ T memory cells are generated in these processes [7]. Therefore, increased numbers of experimental vaccines have been focused in creating molecular networks to initiate and activate the innate and adaptive immune responses [8]. Distinct molecular approaches have been studied to improve the innate immune cell activation by creating local inflammatory niches, followed by lymph

 doi:10.20944/preprints202411.0114.v1

node delivery and induction of robust humoral and cellular response. As known, some vaccines based on antigen/pathogen subunits induce a modest immunogenic response, which justify the use of adjuvant molecules [3], as a tool to increase antigen-specific immune response in quantitative and qualitative terms [4,5].

Among different mechanisms mediated by adjuvants, an important role is the ability to activate innate immune cells, mainly dendritic cells (DCs), increasing antigen uptake, cytokines production and also the higher expression of costimulatory molecules in membrane surface, which is effective to activate and differentiate T cells [9–12]. DCs and other cells of the innate immune system can become activated not only by distinct pathogen associated- molecular patterns (PAMPs) via pattern recognition receptors (PRRs) but also by tissue damage that results in the release of damage-associated molecular patterns (DAMPs) [13–15]. Therefore, DC population exerts a critical role in the recognition of antigen followed by migration to the lymphoid tissue and activation of T cells. DCs interact with T cells mediating 3 signs: 1 –processed antigens presentation in MHC complexes to T lymphocytes through T Cell Receptor (TCR) signaling. 2- expression of costimulatory molecules in the cellular membrane for interacting with ligands expressed in the T cell membrane. 3- production of cytokines as mediators of T cell effector polarization [16–18].

Aluminum salts are the most common adjuvants licensed [19]. Concerning the growth of nanotechnology research, nanostructures are widely studied for vaccine design, mainly as adjuvant tools [13]. Nanoparticles such as liposomes, microspheres, chitosan-nanoparticles and polymers have been evaluated as potent antigen carriers able of immune-adjuvant activity [15,16,20–22]. Immunomodulatory properties of cationic polymers such as chitosan and poly (ethylene imine) (PEI) have been investigated aiming at vaccine development. Carroll et al. (2016) showed the ability of chitosan to induce BM-DCs maturation in an IFN-I-dependent manner, consequently providing cyclic GMP-AMP synthase (c-GAS) and Stimulator of Interferon Genes (STING) dependent Th1 immunity [23]. The adjuvanticity of PEI and PEI-based particles has been correlated with the ability to generate danger signals that mediate the immune cells activation as APCs and induction of adaptive responses [24]. Pérez-Betancourt and collaborators (2020) demonstrated that poly (diallyl dimethyl ammonium chloride), PDDA, conjugated to OVA (OVA/PDDA NPs) were 170 nm in hydrodynamic diameter, displayed high colloidal stability, low polydispersity and positive zeta potential (+30 mV) inducing a robust anti-OVA IgG1 and IgG2a antibody production, as well as T cell response in immunized mice such as verified by the compared immunization with OVA and Alum [25]. The present data further reinforce the important role that cationic polymers can have in vaccine design. Herein the *in vitro* and *in vivo* experiments show that OVA/PDDA-NPs induced a potent anti-OVA antibody response, as previously demonstrated by Pérez-Betancourt et al. (2020) [25]. Furthermore, higher numbers of plasma cells and memory B cells were also verified in mice immunized with OVA/PDDA-NPs compared with OVA/Alum immunization. OVA/PDDA-NPs induced DCs maturation and also migration to draining lymph nodes. Higher uptake of OVA/PDDA-NPs compared with soluble OVA by immature DCs was also verified resulting in T cell response. DCs incubated *in vitro* with OVA/PDDA-NPs were also able to significantly improve OVA-specific $CD4^+$T cell proliferation. Taken together, OVA/PDDA-NPs exert a direct effect on DCs leading to their maturation and consequent development of $CD4^+$T cell response that potentiates antibody production and generation of memory B cells.

2. Materials and Methods

2.1. Antigens and Adjuvants

Ovalbumin grade V (OVA- Sigma-Aldrich) was used in the *in vivo* and *in vitro* experiments. For the *in vitro* protocols, Lipopolysaccharide (LPS, E. coli-Sigma- Aldrich) was used in association with OVA. Aluminum hydroxide-Alum (Sanofi) was adsorbed to OVA and used in the *in vivo* immunization of mice. OVA/PDDA NPs. The process of OVA/PDDA-NPs formulation was confirmed by the measurement of turbidity of the dispersion and monitored in a Beckman

 doi:10.20944/preprints202411.0114.v1

spectrophotometer at 300 nm. OVA-FITC (Invitrogen) or conjugated to PDDA (OVA-FITC/PDDA) was used in *in vitro* experiments.

2.2. Experimental Groups

For experimental procedures, isogenic BALB/c male mice (7-8 weeks) were obtained from Central Bioterium (Butantan Institute) and DO11.10 mice (7-8 weeks) were obtained from Laboratory of Animal Facility (ICB/USP). The BALB/c mice were maintained in the Immunopathology Laboratory facility while DO11.10 mice were maintained in the Special Laboratory of pain and signaling of Butantan Institute under controlled temperature, 12/12 light/dark and standard feed and water *ad libitum*. The current study was conducted after ethical committee approval (CEUAIB: 1282081119).

2.3. Endotoxin Removal in OVA and Protein Concentration Experiment

Samples of OVA diluted in water (25 mg/mL) were submitted to a polymyxin column immobilized on Sepharose, (Thermo Scientific), to remove possible LPS contamination. Afterwards, the protein content was determined by the BCA bicinchoninic acid method (Sigma-Aldrich).

2.4. Preparation of PDDA/OVA Dispersions

Stock solutions of OVA (10 mg/mL) and PDDA (1 mg/mL) were used to obtain the OVA/PDDA-NPs. Therefore, the NPs were prepared using 100 μg/mL of OVA with 10 μg/mL of PDDA in D.I water as previously shown by Pérez-Betancourt et al. (2020) [25]. After 30 minutes OVA/PDDA-NPs formation was monitored by turbidity analysis by measuring the optical density at 300 nm in a spectrophotometer (Beckman). For the experiments, only dispersions with optical density above 0.300.

2.5. Confirmation of the Mean Hydrodynamic Diameter of NPs by Dynamic Light Scanning (DLS) and Zeta Potential

The average hydrodynamic diameter of the NPs together with the evaluation of the polydispersion index (PdI) was performed by dynamic light scattering (DLS) and Zeta-potential using 2 mL of sample in the Zeta Plus Zeta Potential Analyzer equipment.

2.6. Ultracentrifugation of OVA/PDDA-NPs

Samples of OVA/PDDA-NPs prepared as previously described and soluble OVA (100 μg/mL) were centrifuged at 14,500 rpm for 30 minutes. After that, the supernatants (SBNs) were collected and the protein content was determined by BCA.

2.7. Immunization Protocol

Groups of BALB/c male mice (aged 7-8 weeks) were immunized with 200 μL of OVA/PDDA-NPs (100 μg/10 μg/mL) or OVA/Alum (100 μg/100 μg/mL) via subcutaneously (s.c.) in the base of the tail. After 21 days, the mice groups received antigenic booster s.c. Group of non-immunized mice received 200 μL of water at the same route and used it as control.

2.8. Analysis of Plasma Cell and Memory B Cell Populations in Splenocyte Suspensions from Non-Immunized or Immunized Mice with OVA/Alum and OVA/PDDA-NPs

On day 28 after immunization, splenocyte suspensions were prepared from non-immunized or immunized mice. Spleens were collected and macerated, in a sterile environment. After, red cells were lysed with a lysis buffer for 3 minutes in 4°C and the number and viability of the cells determined by counting in a Neubauer chamber with a 0.1% Trypan Blue solution. The cell suspensions were incubated with Fcγ block mAb (1μg/10^6 cell) for 15 min at 4^o C. Afterwards,

 doi:10.20944/preprints202411.0114.v1

samples of $2x10^6$ cells diluted in 100 µL of PBS buffer were distributed in 96-well plates (Corning) and incubated with fixable viability staining (FVS) 510 (BD Biosciences) for 15 minutes at room temperature (RT). Subsequently, the cell samples were washed with PBS + 1% FBS buffer followed by centrifugation. The cells were resuspended and incubated with monoclonal antibodies anti-surface markers of memory B cell (anti-CD19 PE, anti-CD27 BV421, and anti-CD38) and plasma cell (PC) (anti-CD19 APC and Anti-CD138 BV421).

Samples were acquired (50,000 events) by FACsCanto II and analyzed by FlowJo Software. Parameters of size and granularity were selected, followed by "Single Cell" and selection of viable cells using FVS marking (FSC-A/AmCyamA). From the viable cell population, the double-labeled CD19+CD138+ cell populations (plasma cells) were selected and, from the CD19+ population, the analysis of the double-labeled CD27+CD38+ population (memory B cells) was performed. For the analysis, the fluorescence-minus-one (FMO) methodology was used. Analyzes were performed on samples obtained from individual animals (n=4). Results were expressed as the mean absolute cell number of individual animals/group ± Standard Deviation (SD).

2.9. Analysis of the Expression of MHC Class II and Costimulatory Molecules in DCs from Cell Suspensions Obtained from Non-Immunized Mice or Mice Immunized with OVA/Alum or OVA/PDDA

Mice were immunized with OVA/Alum or OVA/PDDA. After 2, 3 and 4 days of immunization, cell suspensions were prepared from inguinal lymph nodes. Suspensions were resuspended in PBS + 1% FBS and were distributed in 96-well plates (Corning) and incubated with anti-CD11c PE.Cy7, anti-MHC II FITC and costimulatory labeled fluorophores: CD80 APC and CD40 BV421. Samples were fixed in PBS+ 1% formaldehyde (Merck). Samples were acquired in a FacsCanto II flow cytometer (BD Bioscience) and analyzed in FlowJo software. Analyzes were performed on samples obtained from individual animals (n=4-5). The analysis strategy was initiated by the parameters FSC-A x SSC-A, followed by the exclusion of clustered cells (FSC-A x FSC-H) and the selection of the population of live cells by marking with FVS. Then, the population of $CD11c^+$ cells was analyzed and, from this cell population, the expression of molecules of MHC-II, CD40, CD80 and CD86 in mean fluorescence intensity (MIF) was analyzed. For the analysis, the fluorescence-minus-one (FMO) methodology was used. Results were expressed as the mean absolute cell number of individual animals/group ± Standard Deviation (SD) or the MFI of MHC molecules or costimulatory expression of individual animals/group ± SD.

2.10. Differentiation of DCs from Bone Marrow (iBM-DCs) of BALB/c Mice

The femur of BALB/c mice were collected using surgical kit in a sterile environment. The femoral cavity was washed with non-supplemented RPMI-1640 medium until complete removal of all bone marrow. The cell counter in suspension was determined using Neubauer chamber and 0.1% of Trypan Blue solution. Suspensions of $30x10^6$ cells were distributed in culture bottles in 20 mL in RPMI medium supplemented with 1% L-glutamine, 0.5% 2-mercaptoethanol, 1% penicillin-streptomycin, 1% vitamin and 5% FBS plus 10 ng/mL of GM-CSF and 5 ng/mL of IL-4 and maintained at 5% CO_2/ 37 °C. On day 4 of culture, the medium is replaced and on the 7th day, the cells in suspension were collected and counted in the Neubauer chamber to carry out the *in vitro* experimental tests.

2.11. In Vitro Experiment of iBM-DCs Stimulated with OVA, OVA/LPS or OVA/PDDA-NPs

iBM-DCs ($3x10^6$) were maintained in supplemented RPMI medium or incubated with OVA (100 µg/mL), OVA/PDDA (100/10µg/mL) and OVA/LPS (100 µg/mL/250 ng/mL) for 18 h/37° C. After this period, the cells were collected for analysis of MHC-II, CD40, CD80 and CD86 expression by flow cytometry. The culture supernatants were used for detection of IL-10, IL-12 and TNF-α by ELISA.

Suspensions of $1x10^6$/cells were labeled with the Fixable viability stain (FVS) 510 (BD Biosciences) diluted in PBS for 15 min/R.T. After the FVS labeling, after, DCs suspensions were stained for 30 min/4°C, with anti-CD80 APC, anti-CD86 PE, anti-MHC-II FITC and anti-CD40 BV421

 doi:10.20944/preprints202411.0114.v1

antibodies labeled with fluorophores, DCs were washed with PBS, centrifuged (1500 rpm/5 min/ 4°C), and fixed with PBS solution +1% paraformaldehyde. The stained cells were read on the BD-FACsCanto II cytometer and analyzed on the FlowJo software. Initially, the analysis and selection of the total population was performed based on the parameters of granularity or internal complexity - Side Scatter area (SSC-A-on the y-axis) versus (vs) relative size, Forward Scatter area (FSC-A-on the y-axis) x), followed by the exclusion of debris and clustered cells, through the analysis of FSC-H in relation to the area of FSC-A. Subsequently, the exclusion of the population of non-viable cells (marked with FVS) was performed, followed by the selection of the population of CD11c+ cells. From this population, the expression of MHC-II molecules or co-stimulators was analyzed. As a parameter to define the populations, the methodology of "fluorescence minus one" (FMO) was used and the results presented as the average of the fluorescence intensity of the costimulatory molecules or MHC II on the population of CD11c+ cells in the samples in triplicates ± SD.

2.12. Evaluation of TNF-α, IL-6, IL-12 and IL-10 Production by ELISA

The TNF-α production was measured using the ebioscience ELISA kit. IL-6 and IL-12 were evaluated by ELISA kits from R&D system. ELISA kits, respectively. The IL-10 was detected by PEPROTECH ELISA Kit. All ELISA assays were performed according to the manufacturer's protocols. The results were calculated by using a standard curve of the recombinant cytokine and the data expressed as the mean of the cytokine concentration of the samples in triplicate ± SD.

2.13. Flow Cytometry Analysis of Binding and Uptake of OVA/PDDA-NPs by iBM-DCs

In order to evaluate the binding of NPs to the DC membrane, as well as the internalization of the OVA/PDDA formulation, the conjugation of OVA-FITC (100 µg/mL) with PDDA (10 µg/mL) was carried out. Samples of BM-DCs ($1x10^6$) were incubated with OVA-FITC/PDDA or OVA-FITC (100 µg/10 µg/mL) for 30 minutes at 4°or 37°C, as described by Favoretto et al. (2017) [26]. All incubations were performed in triplicate. After this period, the cells were washed with PBS and resuspended in 200 µL of PBS with 1% paraformaldehyde. The reading was performed on the FACsCanto II Flow Cytometer and analyzed using the FlowJo software. Results were expressed as Mean Fluorescence Intensity ± SD.

2.14. Analysis of OVA/PDDA-NPs Internalization by Transmission Electron Microscopy (TEM)

Samples of iBM-DCs ($5x10^5$) were incubated for 1h with culture medium, OVA (100 µg/mL) or OVA/PDDA (100 µg/10 µg/mL) at 37 °C. After this period, the cell samples were centrifuged and the pellet was processed. The DC samples were fixed in a 25 % glutaraldehyde and 2 % paraformaldehyde solution in 0.1M cacodylate buffer pH 7.2, for 2 h/RT and washed in the cacodylate buffer 3 times/15 minutes. Subsequently, the post-fixation step was performed in 1% osmium tetroxide in 0.1M cacodylate buffer for 1h followed by washing with the cacodylate buffer 3 times/15 minutes. The pellets were dehydrated in 70 % ethyl alcohol for 10 minutes and the process was repeated once more. Then, the samples were immersed in 95% ethyl alcohol for 15 minutes/2 times and in absolute alcohol 3 times. The samples were incubated with propylene oxide + absolute alcohol in a 1:1 ratio for 15 minutes, twice for 15 minutes in propylene oxide. At the end, the samples were incubated for 2 hours in propylene oxide + resin (1:1). The samples were stored and the next day they were soaked in the resin, subjected to the vacuum chamber for at least 3 times and remained in the oven for 3 days. After performing an ultra-fine cut of the material and its inclusion in a copper screen, the samples were contrasted with uranyl acetate and lead citrate. For contrasting with uranyl acetate, 50 µL of 2% filtered uranyl acetate were added to form a drop on the bench covered with parafilm and the screen was inserted inside the solution drop. After 15 minutes, the material was washed in Milli-Q water at least 50 times and placed to dry on filter paper. For contrasting with lead citrate, the copper screens containing the cells were inserted into a drop of lead citrate previously dripped onto a surface covered with parafilm. After 3 minutes of incubation, the material was washed at least 50

 doi:10.20944/preprints202411.0114.v1

times and placed to dry on filter paper. After contrasting, the images were captured by the TEM 906E Zeiss.

2.15. Antigen-Specific CD4T⁺ Lymphocyte Proliferation Assay

iBM-DCs differentiated according with previously described, were incubated with OVA (100 µg/mL), OVA/PDDA (100 µg/mL) or OVA/LPS (100 µg/mL/ 250 ng/mL) for 18 h/37°C in 5 % humidified CO2. Spleens of DO.11.10 mouse were collected, macerated and incubated with a lysis buffer (3 min/ 4°C). After that, spleen cells were counted in a Neubauer hemocytometer labeled with anti-CD4 PE.Cy-5 (15 min/R.T) and filtered by Cell strain. were purified by cell sorting (FACs Aria). $0.6x10^5$ DCs were co-cultured with $3x10^5$ $CD4^+$ T cells purified by cell sorting from a suspension of lymph node and spleen cells from DO11.10 mice (Figure 12). To evaluate $CD4^+$ T cell proliferation, the co-cultures were incubated for 48 or 72 hours with BrdU (10 µM) at humidified 5 % CO_2 oven. Cell proliferation was evaluated using the BrdU-ELISA kit. All cultures were performed in quadruplicate and results expressed as mean OD ± SD.

2.16. Statistical Analysis

Flow cytometry analyzes were presented by expression of molecules considering the mean fluorescence intensity (MFI) of triplicate samples ± Standard Deviation. Statistical analyses were performed using the One-way ANOVA test, followed by the Tukey method (ZAR, 1984). Differences with $p < 0.05$ were considered statistically significant.

3. Results

3.1. OVA/PDDA Conjugation Produced an Adequate Colloidal Dispersion

To evaluate the adjuvant effect of PDDA in OVA-specific immune response, OVA/PDDA-NPs were prepared, as previously described by Pérez-Betancourt et al., (2020) [25]. Figure 1 shows that the incubation of OVA/PDDA created a turbid colloidal dispersion of a peak of 178 nm (Figure 1A) in agreement with previously reported NPs size in OVA/PDDA water dispersions. Furthermore, after the centrifugation process, OVA was not detected in the supernatant of OVA/PDDA-NPs dispersions in contrast with the centrifuged OVA-solution (Figure 1B).

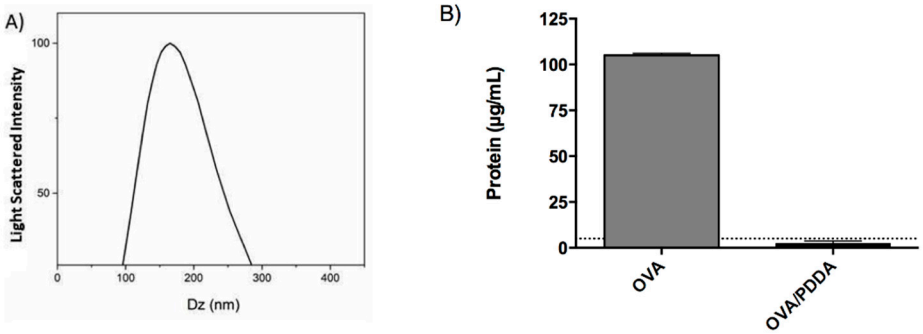

Figure 1. Characterization of OVA/PDDA NPs. (A) hydrodynamic diameter of NPs and (B) protein dosage; (A) After OVA-NPs formation, the hydrodynamic diameter was analyzed by Dynamic Light Scattering (DLS) in ZetaPlus Analyzer. (B) OVA/water (100 µg/mL) or OVA/PDDA (100 µg/10µg/mL) samples were subjected to centrifugation at 14,500 rpm/30 min. Then, the supernatants were collected and the protein concentration determined by the BCA method. The dotted line represents the limit of detection from the BSA standard curve. The results are expressed as the mean of the protein content of samples in quadruplicate ± SD.

 doi:10.20944/preprints202411.0114.v1

3.2. OVA/PDDA Modulates OVA-Specific Adaptive Immune Response in Immunized Mice

Pérez-Betancourt et al., (2020) demonstrated that OVA/PDDA-NPs induced higher DTH and anti-OVA antibody responses when compared with the OVA/Alum-mice group [25]. Our data also showed robust anti-OVA IgG1 and IgG2a antibody production in OVA/PDDA-immunized mice compared with OVA/Alum-group (Figure 2 A-B). Consistently, there was an increase of plasma cells ($CD19^+CD138^+$) in mice immunized with OVA/PDDA or OVA/Alum-groups (Figure 2 C). Reinforcing the potent adjuvanticity of OVA/PDDA-NPs, a higher number of memory B cells ($CD19^+CD38^+CD27^+$) in OVA/PDDA-group was observed in comparison with the OVA/Alum or control-groups (N.I.) (Figure 2 D).

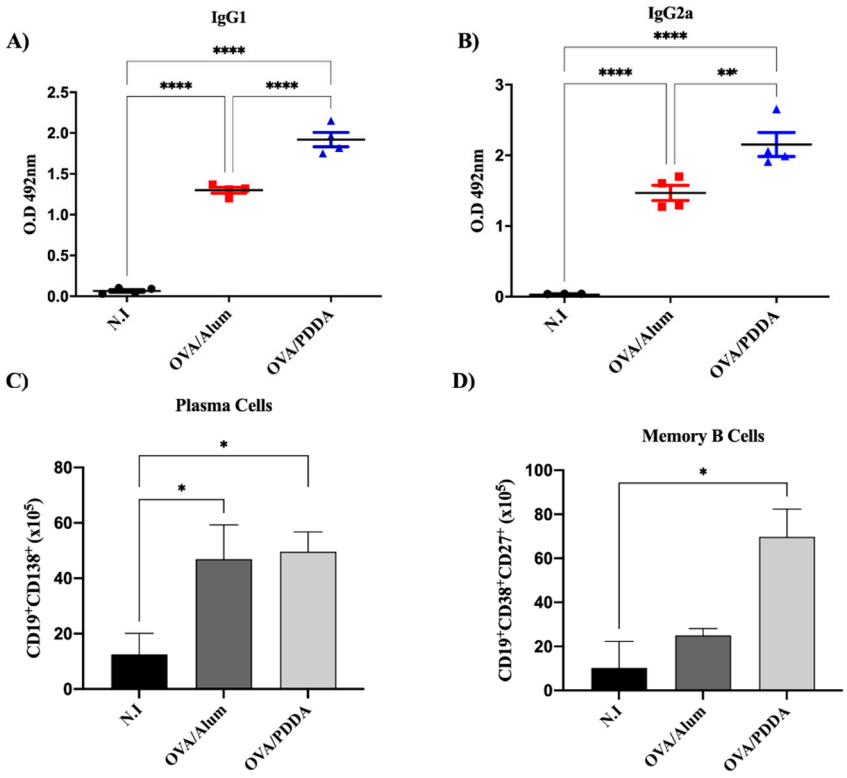

Figure 2. Potent effect of OVA/PDDA-NPs in induction of anti-OVA antibody production and B cell populations. Groups of BALB/c mice were immunized subcutaneously (s.c.) with 200 µL of OVA/Alum (100 µg/100 µg/mL) or OVA/PDDA (100 µg/10 µg/mL). As a control, mice received 200 µL of water. On the 21st day post-immunization, the mice received an antigenic booster and, on day 28 were bled for antibody evaluation, by ELISA. The spleens were also collected to analyze the plasma cell ($CD19^+CD138^+$) and memory B ($CD19^+CD27^+CD38^+$) cell populations by flow cytometry, as described in materials and methods. (A) anti-OVA IgG1 (1/1280) and (B) anti-OVA IgG2a (1/20) antibodies in samples of individual mice/group. The results represent the optical density of the mean of the samples (n=4) ± SD. (C) Number of plasma cells and (D) memory B cells in splenocyte suspensions of the individual mice/group (n=4-5)/group ± SD. * $p < 0.01$ of significance; *** $p < 0.001$ of significance.

3.3. OVA/PDDA-NPs Immunization Increases the Number of $CD11c^+$ Cells Expressing Molecules Involved in Antigen Presentation in Draining Lymphoid Tissue of Mice

DCs have been considered the link between the innate and the adaptive immune response [21]. Therefore, we analyzed this cell population on draining lymph nodes at the first days of OVA/PDDA-NPs immunization. We did not verify DCs migration on draining tissue (data not shown) after OVA/PDDA-NPs or OVA/Alum immunized-groups compared with non-immunized mice.

 doi:10.20944/preprints202411.0114.v1

However, on the 3th day, there was an increase of CD11c⁺ cells in the lymph nodes of OVA/PDDA-NPs group compared with non-immunized (N.I.) or OVA/Alum-mice, as shown on Figure 3 (A). In addition, it was observed upregulation of CD80 and MHC-II expression on CD11c⁺ cells from OVA/PDDA-mice compared with control mice-group. It was also observed higher expression of MHC-II molecules on CD11c⁺ cells of OVA/Alum-group (Figure 3 B-D).

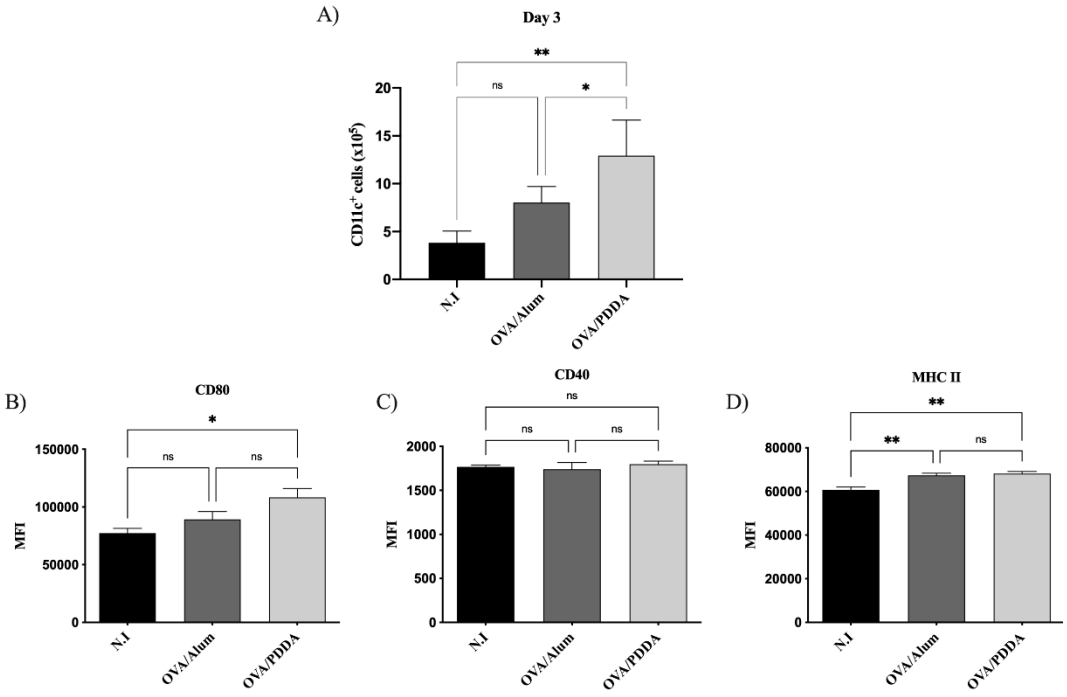

Figure 3. Effect of OVA/PDDA immunization in migration of CD11c$^+$ cells to draining lymph nodes and DCs maturation *in vivo*. Groups of BALB/c mice were immunized (s.c) with 200 µL of OVA/Alum (100 µg/100 µg/mL) or OVA/PDDA (100 µg/10 µg/mL). As a control, mice received 200 µL of water. After 3 days of immunization inguinal lymph nodes were obtained and 1x10^6 cells were incubated with anti-CD11c, anti-CD80, anti-CD40 and anti-MHC II mAb labeled with fluorophores and analyzed by flow cytometry. **(A)** Number of CD11c⁺ cells from mice-groups immunized 3 days before; Expression of **(B)** CD80, **(C)** CD40 and **(C)** MHC-II molecules on CD11c$^+$ cell population from mice groups immunized 3 days before. The analysis strategy is described in material and methods. The results represent the mean of the number of CD11c⁺ cells from lymph node cell suspensions of individual mice/group (n=4) ± SD. Mean of fluorescence intensity (MFI) of molecule expression on CD11c+ cells from individual mice/group (n=4) ± SD. Statistical analysis was performed by one-way ANOVA, with Tukey's post-test. * $p < 0.01$ of significance; ** $p < 0.05$ of significance. Representative results from 3 independent experiments.

Four days after mice immunization, the population of CD11c⁺ cells was increased in draining lymph nodes of the OVA/PDDA-group accompanied by an increased expression of costimulatory and MHC-II molecules on these cells (Figure 4 A- D).

 doi:10.20944/preprints202411.0114.v1

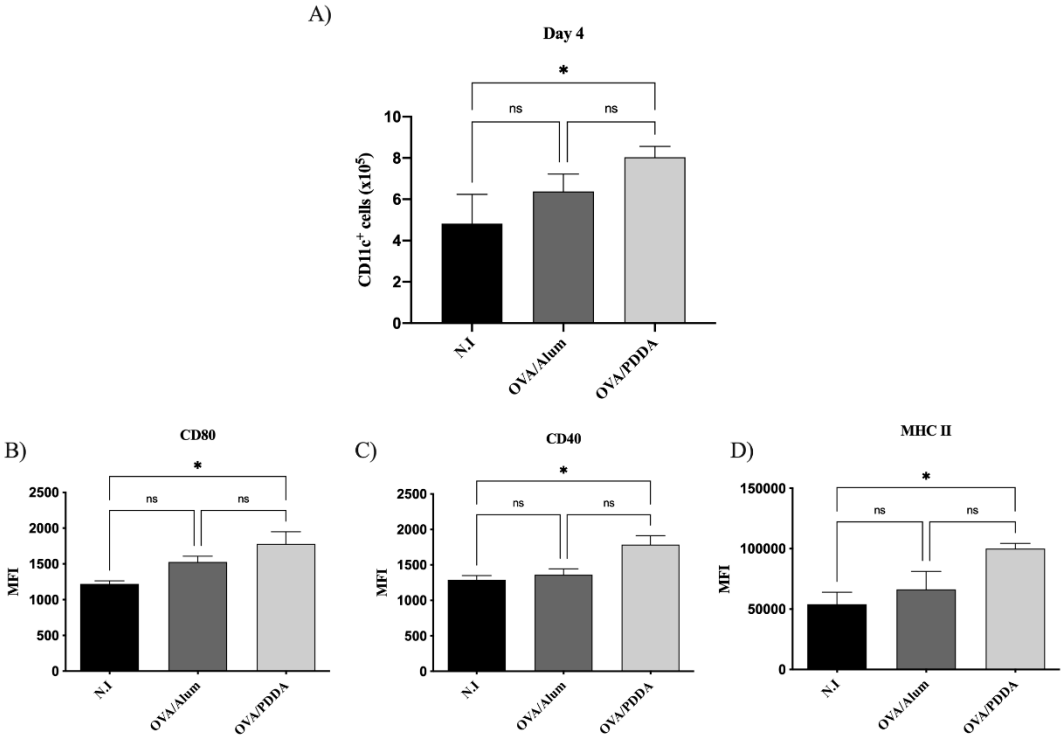

Figure 4. - Effect of OVA/PDDA immunization in migration of CD11c+ cells to draining lymph nodes and DCs maturation *in vivo*. Groups of BALB/c mice were immunized subcutaneously (s.c) with 200 µL of OVA/Alum (100 µg/100 µg/mL) or OVA/PDDA (100 µg/10 µg/mL). As a control, mice received 200 µL of water. After 3 days of immunization inguinal lymph nodes were obtained and 1x10^6 cells were incubated with anti-CD11c, anti-CD80, anti-CD40 and anti-MHC II mAbs labeled with fluorophores and analyzed by flow cytometry. (A) Number of CD11c$^+$ cells from mice-groups immunized 4 days before. Expression of (B) CD80, (C) CD40 and (D) MHC-II molecules on CD11c+ cell population from mice groups immunized 4 days before. The analysis strategy is described in material and methods. The results represent the mean of the number of CD11c+ cells from lymph node cell suspensions of individual mice/group (n=4) ± SD. Mean of fluorescence intensity (MFI) of molecule expression on CD11c+ cells from individual mice/group (n=4) ± SD. Statistical analysis was performed by one-way ANOVA, with Tukey's post-test. * $p < 0.01$ of significance. Representative results from 3 independent experiments.

3.4. OVA/PDDA-NPs Did Not Exert Cytotoxicity on iBM-DCs in Culture

Cationic polymers are known to promote a dose-dependent cytotoxicity [26–28], therefore, it was evaluated the viability of iDCs cultured *in vitro* with OVA/PDDA-NPs (100 µg/10 µg/mL). For this, cultures of iDCs in RPMI medium supplemented with 10%FBS or OPT-MEM medium were incubated with OVA/PDDA-NPs for 24 hours, according to Perez-Betancourt et al., (2020) [25]. The data showed that OVA/PDDA-NPs did not exert cytotoxicity on iDCs (Figure 5).

 doi:10.20944/preprints202411.0114.v1

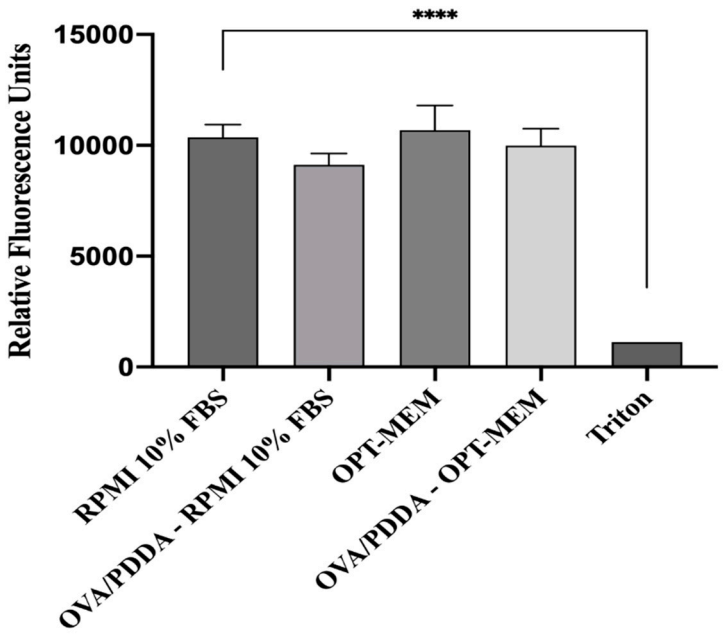

Figure 5. Effect of OVA/PDDA-NPs on viability of BM-DCs in culture. The Presto Blue assay was performed in iBM-DCs cutures incubated with OVA/PDDA-NPs for 24 h in RPMI medium supplemented with 10% FBS or OPT-MEM. Fluorescence was determined by the means of the samples in quadruplicate ± SD. *** $p < 0.001$ of significance.

3.5. Binding and Uptake of OVA/PDDA-NPs by BM-DCs In Vitro

Aiming to understand the potential effect of OVA/PDDA on antigen-presenting cells (APCs), the binding and uptake of NPs by immature Bone Marrow-DCs (iDCs) was determined using OVA-FITC and OVA-FITC/PDDA-NPs incubation at 4 and 37°C, followed analysis by flow cytometry. The internalization of OVA/PDDA-NPs by iBM-DCs was also evaluated by Transmission Electronic Microscopy (TEM). The fluorescence intensity of DCs incubated with OVA-FITC/PDDA was higher than the one of DCs incubated with OVA-FITC at 4°C (Figure 6A) of NPs-binding. Similar results were obtained in iBM-DCs incubated with OVA-FITC or OVA/PDDA-FITC at 37°C (Figure 6B). The figure 7 (G, H and I) shows presence of OVA/PDDA-NPs inside of iBM-DCs observed by TEM, as observed by flow cytometry analysis.

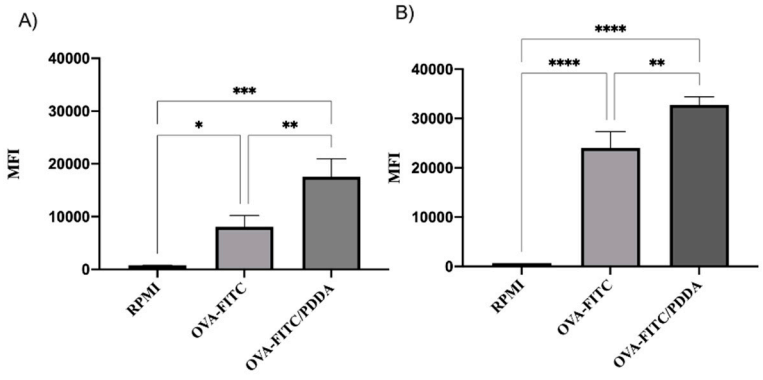

Figure 6. Binding and uptake of OVA-FITC/PDDA and OVA-FITC by iBM-DCs. (A) iBM-DCs were incubated with OVA-FITC or OVA-FITC/PDDA for 30 minutes at 4°C and (B) at 37°C. The samples were analyzed by flow cytometry. Results are expressed as Mean Fluorescence Intensity (MIF) of the samples in triplicate ± SD. * $p < 0.01$ of significance; ** $p < 0.05$ of significance; *** $p< 0.001$ of significance. Representative results of 3 independent experiments.

 doi:10.20944/preprints202411.0114.v1

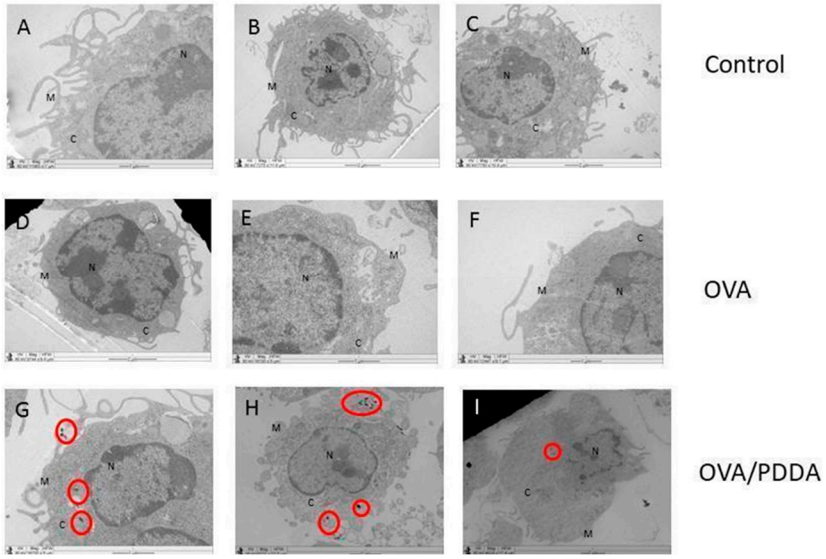

Figure 7. Images of iBM-DCs incubated with OVA or OVA/PDDA by Transmission Electron Microscopy (MET). BM-DCs incubated with OVA or OVA/PDDA for 1 h at 37 °C. (A) RPMI 1640 Medium (B) OVA (100 μg/mL) and (C) OVA/PDDA (100 μg/10 μg/mL). After incubation, samples were collected and prepared for analysis by MET, according to materials and methods. The images were captured using the TEM- LEO 9610 Zeiss, images obtained in magnification of: (A, D and G) magnification of 12930X, (B and E) magnification of 10000x; (D) 9744X, (E) 16700X, (F) 7750X, (G) 16700, (H) 6231X, (I) 4824X. Cell Structures are identified as Membrane (M), Nucleus (N) and Cytosol (C). OVA/PDDA-NPs are identified in the red circles.

3.6. OVA/PDDA-NPs Induced BM-DCs Maturation In Vitro

Considering that the binding and uptake of different antigens are crucial for the DCs maturation and antigen-presentation [30], iBM-DCs were incubated with OVA, OVA/PDDA or OVA/LPS for 18h at 37ºC. Afterwards, the ability of OVA/PDDA-NPs to induce iBM-DCs maturation was analyzed by flow cytometry. OVA/PDDA-NPs upregulated the expression of CD80, CD86, CD40 and MHC-II on DCs, similarly to lipopolysaccharides (LPS) (Figure 8).

 doi:10.20944/preprints202411.0114.v1

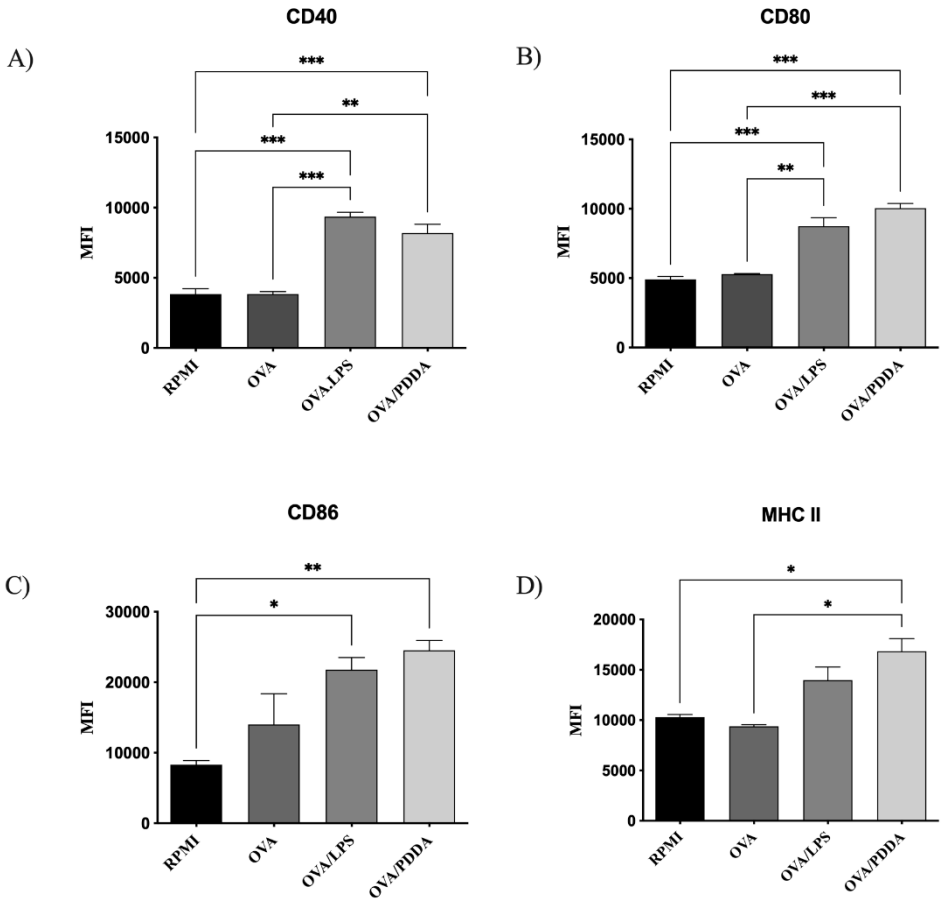

Figure 8. Effect of OVA/PDDA-NPs in the expression of costimulatory and MHC-II on DC culture. iBM-DCs ($1x10^6$) were incubated for 18 h with OVA/LPS, OVA and OVA/PDDA-NPs. After this, the DCs were incubated with anti-CD11c, anti-CD80, anti-CD86, anti-CD40 and anti-MHC II mAbs labeled with fluorophores and analyzed by flow cytometry. The analysis strategy is described in supplementary material. The results represent the mean of fluorescence intensity on $CD11c^+$ cells in triplicate ± SD. * $p < 0.05$ of significance; ** $p < 0.01$ of significance; *** $p < 0.001$ of significance. Representative results from 3 independent experiments.

3.7. OVA/PDDA-NPs Induced Production of Pro-Inflammatory Cytokines by BM-DCs

Production of TNF-α and IL-12 was higher in supernatants of DCs incubated with OVA/PDDA-NPs, OVA or OVA/LPS than DCs incubated with medium only (Figure 9). However, OVA-LPS induced predominantly production of TNF-α by DCs whereas OVA/PDDA increased IL-12 production. Only OVA/LPS stimulated IL-6 production by DCs. IL-10 was not detected by the ELISA assay. Therefore, the production of proinflammatory cytokines, the high expression of co-stimulatory molecules and MHC-II by DCs are strong evidences that OVA/PDDA-NPs are able to induce DCs maturation.

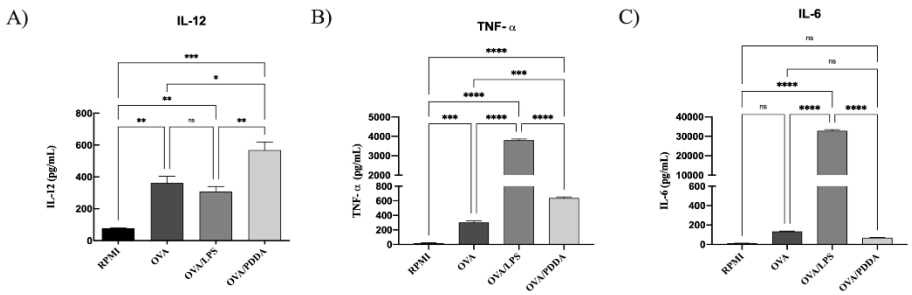

Figure 9. Cytokine production by DCs incubated with OVA/PDDA *in vitro*. iBM-DCs ($1x10^6$) were incubated with OVA, OVA/LPS, or OVA/PDDA for 18 h. Then, the cell supernatants were collected

 doi:10.20944/preprints202411.0114.v1

to detect the cytokines by ELISA. The results represent the mean of the cytokine production in the samples in triplicate ± SD. * $p < 0.05$; ** $p < 0.01$ and *** $p < 0.001$ of significance. Representative results from 2 independent experiments.

3.8. High OVA-Specific CD4$^+$T Cell Proliferation Induced by BM-DCs Incubated with OVA/PDDA-NPs

Since OVA/PDDA-NPs were able to induce DC maturation *in vitro,* we evaluated the ability of these DCs to promote the proliferation of OVA-specific CD4$^+$T cells was evaluated. For this, iBM-DCs were incubated with RPMI medium (control), OVA, OVA/LPS or OVA/PDDA for 18 hours. Afterwards, the DCs were co-cultured with CD4$^+$T cells purified from DO11.10 mice for 72 h.

The results showed that DCs incubated with OVA, OVA/PDDA or OVA/LPS induced a proliferative response of OVA-specific T cells when compared with co-cultures of DCs plus CD4+T cells maintained in culture medium. Furthermore, the proliferative response of CD4+T cells induced by DCs previously incubated with OVA/PDDA was higher than those elicited from co-cultures of CD4$^+$T cells with DCs incubated with OVA (Figure 10).

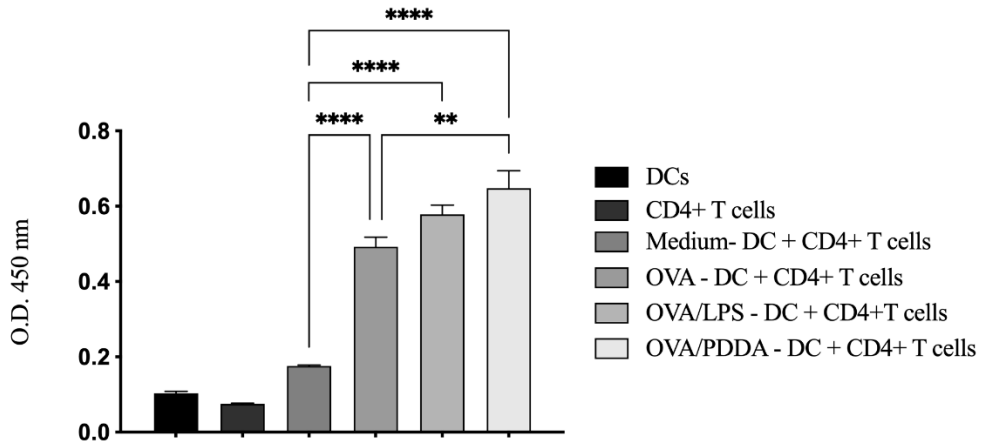

Figure 10. DCs incubated with OVA/PDDA-NPs are able to induce proliferation of OVA-specific CD4+T cells in vitro. iDCs differentiated in vitro were incubated with OVA, OVA/LPS and OVA/PDDA for 18h. After this, the DCs were co-cultured with CD4$^+$ T cells purified from DO11.10 mice for 72 h. The proliferative response was evaluated using BrdU-ELISA assay. Results expressed as the mean of optical density obtained in samples in quadruplicate ± SD. * $p<0.05$ co-cultures of DCs incubated with OVA/LPS, OVA or OVA/PDDA compared with DCs maintained in medium culture (RPMI). ** $p < 0.05$ and **** $p < 0.001$ of significance.

4. Discussion

Pérez-Betancourt et al. (2020) showed that nanoparticles of the cationic polymer poly (diallyl dimethyl ammonium chloride) (PDDA) entangled with OVA elicited high anti-OVA antibody and cellular immune responses in murine model of immunization [31,32]. Therefore, here we clarify the mechanism involved in the induction of antigen-specific immune response elicited by PDDA/OVA NPs water dispersions as mediated by DCs. The physical properties of OVA/PDDA NPs such as size and zeta -potential corroborated those described by Pérez-Betancourt et al (2020) [25]. In addition, no detectable OVA in supernatant of ultra-centrifuged OVA/PDDA dispersions reconfirmed the existence of the OVA/PDDA NPs in the pellets.

The present data also demonstrated that OVA/PDDA-NPs induced high production of OVA-specific IgG1 and IgG2a, as described by Pérez-Betancourt et al. (2020) [25]. Furthermore, here the data add further information on cell populations in mice elicited by OVA/PDDA NPs, namely, increased number of CD19$^+$CD138$^+$ cells and CD19$^+$CD38$^+$CD27$^+$ memory B cells in mice. The generation of memory B cells that are primed to react faster for the antigen/pathogen, with greater intensity and high affinity than in the primary immune response is an important result described in

 doi:10.20944/preprints202411.0114.v1

this work ensuring long-term vaccine efficacy [33,34]. As known, antigen/pathogen-experienced memory B cells represent the second line of defense against homologous challenges that are rapidly reactivated to produce antibodies mediating the immune protection [35,37]. Our data showed that OVA/PDDA-NPs elicited a number of memory B cells ($CD19^+CD38^+CD27^+$ cells) even higher than the one elicited by OVA/Alum immunization, demonstrating the potent effect of the NPs in the induction of a robust antigen-specific immunity. Furthermore, the significant increase of plasma cells ($CD19^+CD138^+$ cells) in OVA/PDDA-NPs mice group is in agreement with the high levels of anti-OVA antibody production detected in our experiments. Importantly, OVA/PDDA-NPs were more efficient in generating memory B cell response in comparison with OVA/Alum. In fact, nanostructures studied in vaccine design are able to modulate immune response [38–40] and the role of innate immunity has been correlated with the efficiency of vaccines to promote an appropriate protective immune response [41].

DCs have a functional plasticity participating in either adaptive immune induction or tolerance process [42]. In immature state, DCs are situated in the periphery, strategically recognizing and capturing antigens. Upon antigen stimulation, DCs migrate to lymphoid draining tissue, present processed peptides derived from captured antigens complexed with major histocompatibility complex (MHC) and costimulatory molecules and secrete cytokines to promote T cells activation and differentiation [43]. The analysis of the CD11c+ cells in our murine immunization model showed higher number of this cell population induced by OVA/PDDA-NPs or OVA/Alum in comparison with naïve mice. Furthermore, $CD11c^+$ cells with upregulated expression of MHC-II and costimulatory molecules were significantly induced by OVA/PDDA-NPs, similarly to gold NPs (Au-NPs), as a vaccine delivery agent with distinct antigens [42]. Therefore, the results demonstrate the ability of OVA/PDDA-NPs to upregulate the DC maturation and migration to lymphoid tissue clarifying how OVA/PDDA NPs activated innate immunity. Furthermore, the data demonstrated the uptake of OVA/PDDA dispersions by DCs and also its ability to potentiate the functional activity of DCs to induce OVA-specific $CD4^+$T cell proliferation.

In *in vitro* assays using BM-DCs, the conjugation of OVA with PDDA promoted an increase of binding and uptake of OVA/PDDA-NPs by iBM-DCs compared with OVA-solution as depicted from fluorescence-labelled OVA analyzed by flow cytometry. Different cellular entry routes are available for nanoparticles during *in vivo* and *in vitro* cell exposure, some evidences reinforce that cationic NPs bind to lipid bilayers and can enter in cells by endocytosis or direct translocation, however the exact way NPs gain access into cells is under investigation [45,46]. Here the presence of OVA/PDDA-NPs in the cytosol of DCs was evidenced by TEM. In agreement with the present results, Chang and colleagues (2017) [47] previously demonstrated by flow cytometry and microscopy that OVA/PDDA-NPs of different sizes were more internalized by DCs when compared to soluble-OVA.

In addition, it was verified the ability of the OVA/PDDA-NPs immunization to promote the migration and maturation process of DCs to lymphoid tissues of the mice. Furthermore, the data also showed that OVA/PDDA-NPs promoted the enhancement of DCs expressing MHC-class II and molecules involved antigen-presenting, as well as the cytokine secretion *in vitro*, which mediate $CD4^+$T cell activation and differentiation for effector cells. DCs previously incubated with OVA/PDDA-NPs also induced highest $CD4^+$T cell proliferation when compared with DCs incubated with OVA/LPS or soluble-OVA *in vitro*.

In accordance with our data, Xu et al. (2012) studding gold nanostructures of cetyltrimethylammonium bromide (CTAB), poly(diallyl dimethyl ammonium chloride) (PDDA), and polyethyleneimine (PEI) combined with HIV-1 Env plasmid DNA (Env) showed the ability of PDDAC-Au NR, PDDAC-Au NR-Env complex, PEI-Au NR or the PEI-Au NR-Env complex, but not CTAB-Au NR or CTAB-Au NR-Env to induce mature DCs ($CD11c^+MHCII^+CD86^+CD80^+$ cells) *in vitro* [48].

Versatile vaccine adjuvants should include memory immunity as our PDDA/OVA NPs do. Our results showed the adjuvant potential of OVA/PDDA-NPs to induce in mice OVA-specific immune response by promoting migration of $CD11c^+$ cells with mature phenotype. In addition, OVA/PDDA-NPs promoted increased expression molecules involved in antigen presentation by DCs, as well as

 doi:10.20944/preprints202411.0114.v1

the production of IL-12 and TNF-α. At last but not least, BM-DCs incubated with OVA/PDDA NPs were able to induce proliferation of OVA-specific $CD4^+$T lymphocytes *in vitro*.

Taken together, the data demonstrate the ability of cationic PDDA/OVA NPs, as adjuvant to protein molecules, to induce a robust adaptive immune response. Corroborating Pérez-Betancourt et al. (2020), our data demonstrate the potential effect of PDDA to promote protein antigen immune response, improving innate immunity activation and consequent adaptive immune response [25]. DCs are the cell type responsible for adaptive immunity induction, and their activation and maturation are required for $CD4^+$ cell response. The binding and uptake increase could be the key for PDDA adjuvant role. In this sense, improvement of DC uptake and binding is an action mechanism reported for different adjuvants [49–51]. The binding can trigger pathways mediated by membrane surface receptors on DCs and consequently the cell maturation. Mature DCs are able to induce T lymphocyte activation and different effector profiles, such as Th1 and Th2 [52]. IgG1 and IgG2a produced by B cells are dependent on the cytokines secreted by Th2 and Th1 profile immune responses. Our results provide evidence on the important ability of PDDA/antigen NPs to strongly elicit antibody-producing B cells.

Cationic nanocarriers are extensively studied as adjuvants for antigenic structures. Lei et al. (2020) evaluated the ability of Chitosan, PEI, DOTAP and the liposome (NeutralL) as adjuvants for SARS-CoV-2 in murine model and the results showed an enhanced immunity in intranasal and intramuscular immunization. the data also showed that the intranasal immunization with PEI promoted higher production of IgG1, IgG2a and IgG2b in mice when compared with the other adjuvants and control groups, while increased production of antibodies was induced by all cationic nanocarriers administered by the intramuscular route. On murine DCs, PEI increased the uptake of antigen by DCs with the release of proinflammatory cytokines. In anti-tumoral vaccines, PEI induced DCs activation with high IL-12 production [53]. Jin and collaborators, (2022) used PEI as adjuvant for antifungal vaccines also showing B cell differentiation for long-lived plasma cells (LLPC) on C57BL/6 mice immunization [54].

In this context, our results show the dynamic of the innate immunity activation targeted by the OVA/PDDA-NPs immunization promoting the maturation of DCs with migration to lymphoid tissue. Furthermore, the data demonstrated the increased uptake of OVA/PDDA-NPs by DCs and also its ability to potentiate the functional activity of DCs to induce OVA-specific $CD4^+$T cell proliferation as a component of adaptive immune response. The robust adaptive immune response induced by OVA-PDDA NPs culminated in significantly increased number of plasma cells and memory B cells in mice.

Supplementary Materials: The following supporting information can be downloaded at the website of this paper posted on Preprints.org.

Author Contributions: Conceptualization, Faquim-Mauro, E.L., Carmona-Ribeiro, AM.; Methodology, Pereira, D.R., Perez-Betancourt Y., Távora B.C.L.F.; Formal Analysis, Pereira, D.R., Faquim-Mauro, E.L., Perez-Betancourt Y., Carmona-Ribeiro, A. M., Távora B.C.L.F. and Magalhães G.S.; Investigation, Pereira, D.R., Faquim-Mauro, E.L., Perez-Betancourt Y. and Távora B.C.L.F; Resources, Faquim-Mauro E.L.; Writing – Pereira, D.R.; Faquim-Mauro E.L., Perez-Betancourt Y., Carmona-Ribeiro, A. M. and Magalhães G.S.; Original Draft Preparation, Pereira, D.R.; Faquim-Mauro E.L., Perez-Betancourt Y. and Távora B.C.L.F; Writing – Review & Editing, Pereira, D.R., Faquim-Mauro, E.L., Perez-Betancourt Y., Carmona-Ribeiro, A. M. and Magalhães G.S.; Supervision, Faquim-Mauro E.L. and Carmona-Ribeiro A. M.; Project Administration, Faquim-Mauro E.L.; Funding Acquisition, Faquim-Mauro E.L.

Funding: This work was supported by Conselho Nacional de Desenvolvimento Científico e Tecnológico (CNPq) by grant 312491/2021-2 to E.L.F.-M. and grant of Coordenação de Aperfeiçoamento de Pessoal de Nível Superior Brasil (CAPES) to D.R.P. for master degree fellowship.

Institutional Review Board Statement: The animal study protocol was approved by the Institutional Ethics Committee of Butantan Institute (protocol code CEUAIB: 1282081119).

Informed Consent Statement: Not applicable.

Data Availability Statement: The original contributions presented in this study are included in this article; further inquiries can be directed to the corresponding author.

Acknowledgments: The authors are grateful to Dr. Dunia Del Carmem Rodriguez Soto from Vaccines Development Laboratory and Dr Luis Sardinha from Butantan Institute facilities for the flow cytometry data acquisition. We thanks for Simone Jared by TEM images acquired in the Butantan Institute facilities.

Conflicts of Interest: The authors declare no conflicts of interest.

References

1. Canouï, E.; Launay, O. [History and principles of vaccination]. *Revue Des Maladies Respiratoires*, **2019,** v. 36, n. 1, p. 74–81.
2. Pollard, A. J.; Bijker, E. M. A guide to vaccinology: from basic principles to new developments. *Nature Reviews Immunology*, **2020**, v. 21, n. 21, p. 1–18.
3. Awate, S.; Babiuk, L. A.; Mutwiri, G. Mechanisms of Action of Adjuvants. *Frontiers in Immunology*, **2013**, v. 4, n. 114.
4. Pulendran, B.; S. Arunachalam, P.; O'hagan, D. T. Emerging concepts in the science of vaccine adjuvants. Nature *Reviews Drug Discovery*, **2021**, v. 20, n. 6, p. 454–475.
5. Canouï, E.; Launay, O. [History and principles of vaccination]. *Revue Des Maladies Respiratoires*, 2019, v. 36, n. 1, p. 74–81.
6. Kondrat C, Hunter C.A. Pathogen interactions with endothelial cells and the induction of innate and adaptive immunity. *Eur J Immunol*. **2018** Oct;48(10):1607-1620. doi: 10.1002/eji.201646789.
7. Bevers S, Kooijmans SAA, Van de Velde E, Evers MJW, Seghers S, Gitz-Francois JJJM, van Kronenburg NCH, Fens MHAM, Mastrobattista E, Hassler L, Sork H, Lehto T, Ahmed KE, El Andaloussi S, Fiedler K, Breckpot K, Maes M, Van Hoorick D, Bastogne T, Schiffelers RM, De Koker S. mRNA-LNP vaccines tuned for systemic immunization induce strong antitumor immunity by engaging splenic immune cells. *Mol Ther*. **2022** Sep 7;30(9):3078-3094. doi: 10.1016/j.ymthe.2022.07.007.
8. Creighton R, Schuch V, Urbanski AH, Giddaluru J, Costa-Martins AG, Nakaya HI. Network vaccinology. *Semin Immunol.* **2020** Aug;50:101420. doi: 10.1016/j.smim.2020.101420.
9. Zhao T, Cai Y, Jiang Y, He X, Wei Y, Yu Y, Tian X. Vaccine adjuvants: mechanisms and platforms. *Signal Transduct Target Ther*. **2023** Jul 19;8(1):283. doi: 10.1038/s41392-023-01557-7.
10. Guimarães LE, Baker B, Perricone C, Shoenfeld Y. Vaccines, adjuvants and autoimmunity. *Pharmacol Res*. **2015** Oct;100:190-209. doi: 10.1016/j.phrs.2015.08.003.
11. Pulendran, B.; Ahmed, R. Immunological mechanisms of vaccination. *Nature Immunology*, **2011**, v. 12, n. 6, p. 509–517.
12. Wang, S.; Suo, X. Still naïve or primed: Anticoccidial vaccines call for memory. Experimental *Parasitology*, **2020**, v. 216, n. 1, p. 107945.
13. Han HJ, Nwagwu C, Anyim O, Ekweremadu C, Kim S. COVID-19 and cancer: From basic mechanisms to vaccine development using nanotechnology. *Int Immunopharmacol*. **2021** Jan;90:107247. doi: 10.1016/j.intimp.2020.107247.
14. Yuen R, Kuniholm J, Lisk C, Wetzler LM. Neisserial PorB immune enhancing activity and use as a vaccine adjuvant. *Hum Vaccin Immunother*. **2019**;15(11):2778-2781. doi: 10.1080/21645515.2019.1609852.
15. Hafner, A. M.; Corthésy, B.; Merkle, H. P. Particulate formulations for the delivery of poly(I:C) as vaccine adjuvant. *Advanced Drug Delivery Reviews*, **2013**, v. 65, n. 10, p. 1386–1399
16. Lee, H.-S.; Jeong, G.-S. Chrysophanol Mitigates T Cell Activation by Regulating the Expression of CD40 Ligand in Activated T Cells. *International Journal of Molecular Sciences*, 2020, v. 21, n. 17, p. 6122.

17. Nel, A. E. T-cell activation through the antigen receptor. Part 1: Signaling components, signaling pathways, and signal integration at the T-cell antigen receptor synapse. *J. Allergy and Clinical Immunology*, **2002**, v. 109, n. 5, p. 758–770.
18. Burkhardt, J. K.; Carrizosa, E.; Shaffer, M. H. The actin cytoskeleton in T cell activation. *Annual Review of Immunology*, **2008**, v. 26, p. 233–259.
19. Del Giudice G, Rappuoli R, Didierlaurent AM. Correlates of adjuvanticity: A review on adjuvants in licensed vaccines. *Semin Immunol*. **2018** Oct;39:14-21. doi: 10.1016/j.smim.2018.05.001.
20. Hamdy S, Haddadi A, Hung RW, Lavasanifar A. Targeting dendritic cells with nano-particulate PLGA cancer vaccine formulations. *Adv Drug Deliv Rev.* **2011** Sep 10;63(10-11):943-55. doi: 10.1016/j.addr.2011.05.021.
21. McCullough KC, Bassi I, Démoulins T, Thomann-Harwood LJ, Ruggli N. Functional RNA delivery targeted to dendritic cells by synthetic nanoparticles. *Ther Deliv*. **2012** Sep;3(9):1077-99. doi: 10.4155/tde.12.90.
22. Pérez-Betancourt Y, Araujo PM, Távora BCLF, Pereira DR, Faquim-Mauro EL, Carmona-Ribeiro AM. Cationic and Biocompatible Polymer/Lipid Nanoparticles as Immunoadjuvants. *Pharmaceutics.* **2021** Nov 4;13(11):1859. doi: 10.3390/pharmaceutics13111859.
23. Carroll EC, Jin L, Mori A, Muñoz-Wolf N, Oleszycka E, Moran HBT, Mansouri S, McEntee CP, Lambe E, Agger EM, Andersen P, Cunningham C, Hertzog P, Fitzgerald KA, Bowie AG, Lavelle EC. The Vaccine Adjuvant Chitosan Promotes Cellular Immunity via DNA Sensor cGAS-STING-Dependent Induction of Type I Interferons. *Immunity*. **2016** Mar 15;44(3):597-608. doi: 10.1016/j.immuni.2016.02.004.
24. Shen C, Li J, Zhang Y, Li Y, Shen G, Zhu J, Tao J. Polyethylenimine-based micro/nanoparticles as vaccine adjuvants. *Int J Nanomedicine*. **2017** Jul 31;12:5443-5460. doi: 10.2147/IJN.S137980. Erratum in: Int J Nanomedicine. 2017 Oct 04;12:7239. doi: 10.2147/IJN.S150593.
25. Pérez-Betancourt Y.; Távora, B. C. L. F.; Colombini M.; Faquim-Mauro E. L.; Carmona-Ribeiro A. M. Simple Nanoparticles from the Assembly of Cationic Polymer and Antigen as Immunoadjuvants. *Vaccines* (Basel). **2020,** v.8 105. 2020.
26. Favoretto BC, Casabuono AAC, Portes-Junior JA, Jacysyn JF, Couto AS, Faquim-Mauro EL. High molecular weight components containing N-linked oligosaccharides of *Ascaris suum* extract inhibit the dendritic cells activation through DC-SIGN and MR. *Mol Immunol*. **2017** Jul;87:33-46. doi: 10.1016/j.molimm.2017.03.015
27. Wang M, Huang H, Sun Y, Wang M, Yang Z, Shi Y, Liu L. PEI functionalized cell membrane for tumor targeted and glutathione responsive gene delivery. *Int J Biol Macromol*. **2024** Jan;255:128354. doi: 10.1016/j.ijbiomac.2023.128354.
28. Salari N, Faraji F, Torghabeh FM, Faraji F, Mansouri K, Abam F, Shohaimi S, Akbari H, Mohammadi M. Polymer-based drug delivery systems for anticancer drugs: A systematic review. *Cancer Treat Res Commun*. **2022**;32:100605. doi: 10.1016/j.ctarc.2022.100605.
29. Gholami L, Mahmoudi A, Kazemi Oskuee R, Malaekeh-Nikouei B. An overview of polyallylamine applications in gene delivery. *Pharm Dev Technol*. **2022** Jul;27(6):714-724. doi: 10.1080/10837450.2022.2107014.
30. Ganem MB, De Marzi MC, Fernández-Lynch MJ, Jancic C, Vermeulen M, Geffner J, Mariuzza RA, Fernández MM, Malchiodi EL. Uptake and intracellular trafficking of superantigens in dendritic cells. *PLoS One*. **2013** Jun 14;8(6):e66244. doi: 10.1371/journal.pone.0066244.
31. Kotsias F, Cebrian I, Alloatti A. Antigen processing and presentation. *Int Rev Cell Mol Biol*. **2019**; 348:69-121. doi: 10.1016/bs.ircmb.2019.07.005.

32. Pérez-Betancourt Y, Távora BCLF, Faquim-Mauro EL, Carmona-Ribeiro AM. Biocompatible Lipid Polymer Cationic Nanoparticles for Antigen Presentation. *Polymers* (Basel). **2021** Jan 7;13(2):185. doi: 10.3390/polym13020185.
33. Carmona-Ribeiro AM. Supramolecular Nanostructures for Vaccines. *Biomimetics* (Basel). **2021** Dec 29;7(1):6. doi: 10.3390/biomimetics7010006.
34. Inoue T, Kurosaki T. Memory B cells. *Nat Rev Immunol*. **2024** Jan;24(1):5-17. doi: 10.1038/s41577-023-00897-3.
35. Sutton HJ, Aye R, Idris AH, Vistein R, Nduati E, Kai O, Mwacharo J, Li X, Gao X, Andrews TD, Koutsakos M, Nguyen THO, Nekrasov M, Milburn P, Eltahla A, Berry AA, Kc N, Chakravarty S, Sim BKL, Wheatley AK, Kent SJ, Hoffman SL, Lyke KE, Bejon P, Luciani F, Kedzierska K, Seder RA, Ndungu FM, Cockburn IA. Atypical B cells are part of an alternative lineage of B cells that participates in responses to vaccination and infection in humans. *Cell Rep.* **2021** Feb 9;34(6):108684. doi: 10.1016/j.celrep.2020.108684.
36. Sutton HJ, Aye R, Idris AH, Vistein R, Nduati E, Kai O, Mwacharo J, Li X, Gao X, Andrews TD, Koutsakos M, Nguyen THO, Nekrasov M, Milburn P, Eltahla A, Berry AA, Kc N, Chakravarty S, Sim BKL, Wheatley AK, Kent SJ, Hoffman SL, Lyke KE, Bejon P, Luciani F, Kedzierska K, Seder RA, Ndungu FM, Cockburn IA. Atypical B cells are part of an alternative lineage of B cells that participates in responses to vaccination and infection in humans. *Cell Rep*. **2021** Feb 9;34(6):108684. doi: 10.1016/j.celrep.2020.108684.
37. Akkaya M, Kwak K, Pierce SK. B cell memory: building two walls of protection against pathogens. *Nat Rev Immunol*. **2020** Apr;20(4):229-238. doi: 10.1038/s41577-019-0244-2.
38. Irvine, D. J.; Read, B. J. Shaping humoral immunity to vaccines through antigen-displaying nanoparticles. *Current Opinion in Immunology*, **2020,** v. 65, p. 1–6.
39. McCraw DM, Myers ML, Gulati NM, Prabhakaran M, Brand J, Andrews S, Gallagher JR, Maldonado-Puga S, Kim AJ, Torian U, Syeda H, Boyoglu-Barnum S, Kanekiyo M, McDermott AB, Harris AK. Designed nanoparticles elicit cross-reactive antibody responses to conserved influenza virus hemagglutinin stem epitopes. *PLoS Pathog*. **2023**, 19(8):e1011514. doi: 10.1371/journal.ppat.1011514.
40. Chang TZ, Stadmiller SS, Staskevicius E, Champion JA. Effects of ovalbumin protein nanoparticle vaccine size and coating on dendritic cell processing. *Biomater Sci.* **2017** Jan 31;5(2):223-233. doi: 10.1039/c6bm00500d.
41. Dong C, Wang Y, Zhu W, Ma Y, Kim J, Wei L, Gonzalez GX, Wang BZ. Polycationic HA/CpG Nanoparticles Induce Cross-Protective Influenza Immunity in Mice. *ACS Appl Mater Interfaces*. **2022** Feb 9;14(5):6331-6342. doi: 10.1021/acsami.1c19192.
42. Leylek R, Idoyaga J. The versatile plasmacytoid dendritic cell: Function, heterogeneity, and plasticity. *Int Rev Cell Mol Biol*. **2019**; 349:177-211. doi: 10.1016/bs.ircmb.2019.10.002.
43. Pishesha, N.; Harmand, T. J.; Ploegh, H. L. A guide to antigen processing and presentation. *Nature Reviews Immunology*, **2022**, v. 22, p. 1–14.
44. Ding L, Yao C, Yin X, Li C, Huang Y, Wu M, Wang B, Guo X, Wang Y, Wu M. Size, Shape, and Protein Corona Determine Cellular Uptake and Removal Mechanisms of Gold Nanoparticles. *Small.* **2018,** Oct;14(42):e1801451. doi: 10.1002/smll.201801451.
45. Donahue, N. D.; Acar, H.; Wilhelm, S. Concepts of nanoparticle cellular uptake, intracellular trafficking, and kinetics in nanomedicine. *Advanced Drug Delivery Reviews*, **2019**, v. 143, p. 68–96.
46. Lin J, Alexander-Katz A. Cell membranes open "doors" for cationic nanoparticles/biomolecules: insights into uptake kinetics. *ACS Nano*. **2013** Dec 23;7(12):10799-808. doi: 10.1021/nn4040553.

47. Chang, T. Z.; Stadmiller, S. S.; Stackevicius, E.; Champion, J. A. Effects of ovalbumin protein nanoparticle vaccine size and coating on dendritic cell processing. *Biomaterial Science*. 2017, v.5 p.223-233.
48. Xu, L.; Liu, Y.; Chen, Z.; Li, W.; Liu, Y.; Wang, L.; Liu, Y.; Wu, X.; Ji, Y.; Zhao, Y.; Ma, L.; Shao, Y.; Chen, C. Surface-engineered gold nanorods: promising DNA vaccine adjuvant for HIV-1 treatment. *Nano letters*, 2012, v. 12, n. 4, p. 2003–2012.
49. Korsholm KS, Agger EM, Foged C, Christensen D, Dietrich J, Andersen CS, Geisler C, Andersen P. The adjuvant mechanism of cationic dimethyldioctadecylammonium liposomes. *Immunology.* **2007,** Jun;121(2):216-26. doi: 10.1111/j.1365-2567.2007.02560.x.
50. Lu Y, Liu ZH, Li YX, Xu HL, Fang WH, He F. Targeted Delivery of Nanovaccine to Dendritic Cells via DC-Binding Peptides Induces Potent Antiviral Immunity *in vivo*. *Int J Nanomedicine*. **2022,** Apr 5;17:1593-1608. doi: 10.2147/IJN.S357462.
51. Marciani DJ. Elucidating the Mechanisms of Action of Saponin-Derived Adjuvants. Trends Pharmacol Sci. 2018 Jun;39(6):573-585. doi: 10.1016/j.tips.2018.03.005.
52. Lei H, Alu A, Yang J, He C, Hong W, Cheng Z, Yang L, Li J, Wang Z, Wang W, Lu G, Wei X. Cationic nanocarriers as potent adjuvants for recombinant S-RBD vaccine of SARS-CoV-2. *Signal Transduct Target Ther.* **2020.** Dec 11;5(1):291. doi: 10.1038/s41392-020-00434-x.
53. Dong H, Wen ZF, Chen L, Zhou N, Liu H, Dong S, Hu HM, Mou Y. Polyethyleneimine modification of aluminum hydroxide nanoparticle enhances antigen transportation and cross-presentation of dendritic cells. *Int J Nanomedicine*. **2018,** Jun 7;13:3353-3365. doi: 10.2147/IJN.S164097.
54. Jin Z, Dong YT, Liu S, Liu J, Qiu XR, Zhang Y, Zong H, Hou WT, Guo SY, Sun YF, Chen SM, Dong HQ, Li YY, An MM, Shen H. Potential of Polyethyleneimine as an Adjuvant To Prepare Long-Term and Potent Antifungal Nanovaccine. *Front Immunol*. **2022** May 16;13:843684. doi: 10.3389/fimmu.2022.843684.
55. Rasband, W.S., ImageJ, U. S. National Institutes of Health, Bethesda, Maryland, USA, https://imagej.nih.gov/ij/, 1997-2018.
56. Wen, H., Qu L., Zhang Y., Xu B., Ling S., Liu X., Luo Y., Huo D., Li, W., Yao X. A Dendritic Cells-Targeting Nano-Vaccine by Coupling Polylactic-Co-Glycolic Acid-Encapsulated Allergen with Mannan Induces Regulatory T Cells. *Int Arch Allergy Immunol*., **2021** v.182 p.777-787.